New Magic Formula Demonstration Shows Unexpected Features of Geometrically Defined Matrices for Polyhedral Grids

Silvano Pitassi [1], Riccardo Ghiloni [2], and Ruben Specogna [1]

[1]EMCLab, Polytechnic Department of Engineering and Architecture, University of Udine, 33100 Udine, Italy
[2]Department of Mathematics, University of Trento, 38122 Trento, Italy

Magic formulas are the geometric identities at the root of modern compatible schemes for polyhedral grids. We present rigorous yet elementary proofs of the magic formulas originating from Stokes theorem. The proofs enlighten new fundamental aspects of the mass matrices produced with the magic formulas. First, the construction of the mass matrices works for an unexpectedly broad type of mesh cells. Second, they show that dual nodes can be arbitrarily positioned thus extending the construction of the dual barycentric grid.

***Index Terms*—Compatible methods, geometrically defined mass matrices, magic formula, polyhedral mesh.**

I. Introduction

The magic formulas, introduced in [1] and [2], enable a simple mapping of *degrees of freedom* (DoFs) attached to edges and faces to a constant vector field.

Magic formulas are at the root of modern compatible or mimetic schemes [3], [4]. They play a major role in the construction of *discrete Hodge operators* [5], and their corresponding algebraic realization given by *mass matrices* [6]. Here, a well-established design strategy decomposes local mass matrices as the sum of a *consistent* and a *stabilization* term [7]. Such a decomposition of the local mass matrix is suggestive since each term plays a specific role, namely, the consistent term, that is constructed starting from magic formulas, enforces a *polynomial consistency* property, while the stabilization term ensures positive-definiteness, preserving the consistency already achieved [4]. In addition, magic formulas have broader applicability than the construction of mass matrices. As an instance, they can be used to reconstruct the vector fields for postprocessing and imaging purposes.

In this work, we present novel proofs of the magic formulas using Stokes theorem. The proofs enlighten new fundamental aspects of the mass matrices produced with the magic formulas. First, the construction of the mass matrices works for an unexpectedly broad type of mesh cells, thus debunking the conventional wisdom that mesh cells have to be star-shaped [2], [4]. Second, it extends the construction of the dual grid [6], [8] in the discretization since it shows that dual nodes can be arbitrarily positioned, even outside the single mesh cell.

II. Geometry of Primal and Dual Grid

Without losing generality, we will focus on a grid consisting of a single polyhedral cell c, Fig. 1(a). To describe the geometric elements of the pair of grids, we introduce a Cartesian system of coordinates with the specified origin and we denote by $\boldsymbol{x} = (x_1, x_2, x_3)^{\mathrm{T}}$ the coordinates of its generic point.

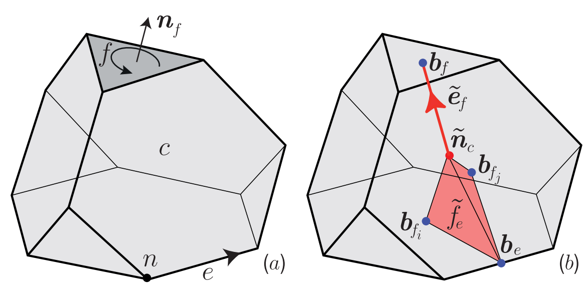

Fig. 1. (a) Primal and (b) dual geometric elements of a polyhedron $c \in C$.

The geometric elements of the primal grid are *nodes* $\boldsymbol{n}$, *edges* e, *faces* f, and the *cell* c itself. The geometric elements of the primal grid are provided with an inner orientation [8].

Now, a *dual grid* is introduced; each geometric entity of the dual grid is in one-to-one correspondence with a geometric element of the primal grid and it is constructed by means of the *barycentric subdivision* [8] of the primal grid. Therefore, the dual of a primal cell c is the dual node $\tilde{\boldsymbol{n}}_c$, where symbol "$\sim$" denotes geometric elements of the dual grid; similarly, the dual of a primal edge e is the dual face $\tilde{f}_e$ and the dual of a primal face f is the dual edge $\tilde{e}_f$, Fig. 1(b)

Precisely, a dual node $\tilde{\boldsymbol{n}}_c$ coincides with the barycenter $\boldsymbol{b}_c$ of a cell c; a dual edge $\tilde{e}_f$ joins $\tilde{\boldsymbol{n}}_c$ with the barycenter $\boldsymbol{b}_f$ of a primal face f; a dual face $\tilde{f}_e$ is a quadrilateral surface made of a union of a pair of triangles; the first has the vertices $\tilde{\boldsymbol{n}}_c, \boldsymbol{b}_e, \boldsymbol{b}_{f_i}$, the second has vertices $\tilde{\boldsymbol{n}}_c, \boldsymbol{b}_e, \boldsymbol{b}_{f_j}$, with f_i, f_j the two faces such that $e = f_i \cap f_j$, with $i = i(e)$ and $j = j(e)$.

Dual edge $\tilde{e}_f$ and dual face $\tilde{f}_e$ are endowed with outer orientation [8], in such a way that each of the pairs $(e, \tilde{f}_e)$, $(f, \tilde{e}_f)$ is oriented according to the right-hand rule.

To each of the following geometric elements e, f, $\tilde{f}_e$, $\tilde{e}_f$ of the primal or of the dual grid, we associate their corresponding vectors $\boldsymbol{e}$, $\boldsymbol{f}$, $\tilde{\boldsymbol{f}}_e$, $\tilde{\boldsymbol{e}}_f$ respectively. Any of these vectors will be represented with a column array of its Cartesian components. Vector $\boldsymbol{e}$ is the edge vector associated with edge e; for example,

Manuscript received November 30, 2020; revised March 1, 2021; accepted March 16, 2021. Date of publication March 19, 2021; date of current version May 17, 2021. Corresponding author: S. Pitassi (e-mail: silvano.pitassi@gmail.com).

Color versions of one or more figures in this article are available at https://doi.org/10.1109/TMAG.2021.3067438.

Digital Object Identifier 10.1109/TMAG.2021.3067438

$\boldsymbol{e} = \boldsymbol{n}_i - \boldsymbol{n}_j, i \neq j$, where $\boldsymbol{n}_i$ and $\boldsymbol{n}_j$ are the coordinates of the boundary nodes of $\boldsymbol{e}$. $\boldsymbol{t}_e$ represents the unit vector of $\boldsymbol{e}$ in such a way that $\boldsymbol{e} = |e|\boldsymbol{t}_e$, where $|e|$ denotes the length of e. Vector $\boldsymbol{f}$ is the face vector associated with face f defined as $\boldsymbol{f} = |f|\boldsymbol{n}_f$, where $\boldsymbol{n}_f$ is the unit normal vector orthogonal to f and $|f|$ denotes the area of f. In a similar way, vector $\tilde{\boldsymbol{e}}_f$ is the edge vector associated with the dual edge $\tilde{e}_f$; for instance, $\tilde{\boldsymbol{e}}_f = \boldsymbol{b}_f - \tilde{\boldsymbol{n}}_c$, see Fig. 1(b). Vector $\tilde{\boldsymbol{f}}_e$ is the face vector associated with the dual face $\tilde{f}_e$. Face vector $\tilde{\boldsymbol{f}}_e$ is equal to $\tilde{\boldsymbol{f}}_e = \frac{1}{2}\big(\tilde{\boldsymbol{e}}_{f_i} \times (\boldsymbol{b}_e - \tilde{\boldsymbol{n}}_c) - \tilde{\boldsymbol{e}}_{f_j} \times (\boldsymbol{b}_e - \tilde{\boldsymbol{n}}_c)\big)$ with f_i, f_j two faces such that $e = f_i \cap f_j$, with $i = i(e)$ and $j = j(e)$, and in such a way that the expression induces the correct orientation on $\tilde{\boldsymbol{f}}_e$, see Fig. 1(b).

III. The Magic Formulas and Their Proofs

Let us consider a pair of vector fields $\boldsymbol{u}, \boldsymbol{w} : \mathbb{R}^3 \to \mathbb{R}^3$ along with a scalar field $w : \mathbb{R}^3 \to \mathbb{R}$ defined on a given cell c. The following well-known integration by part formulas hold

$$\int_c \boldsymbol{u} \nabla \cdot w \, dV = -\int_c \nabla \cdot \boldsymbol{u} \, w \, dV + \int_{\partial c} \boldsymbol{u} \cdot \boldsymbol{n} \, w \, dS \tag{1}$$

$$\int_c \boldsymbol{u} \cdot \nabla \times \boldsymbol{w} \, dV = \int_c \nabla \times \boldsymbol{u} \cdot \boldsymbol{w} \, dV + \int_{\partial c} \boldsymbol{u} \times \boldsymbol{n} \cdot \boldsymbol{w} \, dS. \tag{2}$$

Given a cell c, we denote by $|c|$ its volume. We write "$f \in \partial c$" meaning that f is varying over all (oriented) faces of c. Similarly, we write "$e \in \partial c$" meaning that e varies over all (oriented) edges of c. Finally, given a polygon f in some (affine) plane of $\mathbb{R}^3$, we write "$e \in \partial f$" meaning that e varies over all (suitably oriented) edges of the boundary of f.

Theorem 1 (Reconstruction From Face DoFs): Let $\boldsymbol{u}$ be a constant vector field defined on a cell c. Choose an arbitrary dual node $\tilde{\boldsymbol{n}}_c \in \mathbb{R}^3$ and define $\tilde{\boldsymbol{e}}_f := \boldsymbol{b}_f - \tilde{\boldsymbol{n}}_c$ as at the end of Section II. The following equality holds:

$$\boldsymbol{u} = \frac{1}{|c|} \sum_{f \in \partial c} (\boldsymbol{u} \cdot \boldsymbol{f}) \, \tilde{\boldsymbol{e}}_f. \tag{3}$$

Proof: Let $\boldsymbol{w} \in \mathbb{R}^3$. Thanks to (1), we have

$$\begin{aligned} |c| \, \boldsymbol{u} \cdot \boldsymbol{w} &= \int_c \boldsymbol{u} \cdot \boldsymbol{w} \, dV \\ &= \int_c \boldsymbol{u} \cdot \nabla(\boldsymbol{w} \cdot (\boldsymbol{x} - \tilde{\boldsymbol{n}}_c)) \, dV \\ &= \int_{\partial c} (\boldsymbol{u} \cdot \boldsymbol{n}) \, (\boldsymbol{w} \cdot (\boldsymbol{x} - \tilde{\boldsymbol{n}}_c)) \, dS \\ &= \sum_{f \in \partial c} (\boldsymbol{u} \cdot \boldsymbol{f}) \, ((\boldsymbol{b}_f - \tilde{\boldsymbol{n}}_c) \cdot \boldsymbol{w}). \end{aligned} \tag{4}$$

By using the definition of $\tilde{\boldsymbol{e}}_f$, it follows that

$$|c| \, \boldsymbol{u} \cdot \boldsymbol{w} = \sum_{f \in \partial c} (\boldsymbol{u} \cdot \boldsymbol{f}) \, (\tilde{\boldsymbol{e}}_f \cdot \boldsymbol{w}). \tag{5}$$

Since $\boldsymbol{w}$ is arbitrary, we obtain the claimed equality. □

Lemma 1 (Reconstruction From Edge DoFs Restricted to a Polygonal Face): Let $\boldsymbol{u}$ be a constant vector field, and let f be a polygon in some plane L of $\mathbb{R}^3$ (Fig. 2). Let us denote

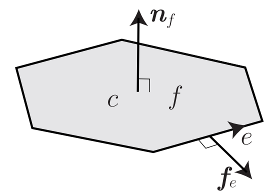

Fig. 2. Polygon and the relevant geometric elements involved in the proof of Lemma 1.

with $\boldsymbol{n}_f$ the unit normal vector orthogonal to f. Choose an arbitrary point $\boldsymbol{p} \in \mathbb{R}^3$. The following equality holds:

$$\boldsymbol{u} \times \boldsymbol{n}_f = \frac{1}{|f|} \sum_{e \in \partial f} (\boldsymbol{u} \cdot \boldsymbol{e}) \, (\boldsymbol{b}_e - \boldsymbol{p}). \tag{6}$$

Proof: Let $\boldsymbol{f}_e := \boldsymbol{e} \times \boldsymbol{n}_f$ be the vector orthogonal to edge e in L. Note that vector $\boldsymbol{u} \times \boldsymbol{n}_f$ belongs to L. Thus, if we apply the argument used in the proof of Theorem 1 to the vector field $\boldsymbol{u} \times \boldsymbol{n}_f$ restricted to f, then we obtain

$$\boldsymbol{u} \times \boldsymbol{n}_f = \frac{1}{|f|} \sum_{e \in \partial f} ((\boldsymbol{u} \times \boldsymbol{n}_f) \cdot \boldsymbol{f}_e) \, (\boldsymbol{b}_e - \boldsymbol{p}). \tag{7}$$

Based on the definition of $\boldsymbol{f}_e$, it follows that

$$(\boldsymbol{u} \times \boldsymbol{n}_f) \cdot \boldsymbol{f}_e = (\boldsymbol{u} \times \boldsymbol{n}_f) \cdot (\boldsymbol{e} \times \boldsymbol{n}_f) \tag{8}$$

$$= (\boldsymbol{n}_f \times (\boldsymbol{u} \times \boldsymbol{n}_f)) \cdot \boldsymbol{e} = \boldsymbol{u} \cdot \boldsymbol{e} \tag{9}$$

and hence, substituting in (7), we obtain the claimed equality. □

Theorem 2 (Reconstruction From Edge DoFs): Let $\boldsymbol{u}$ be a constant vector field defined on a cell c. Choose an arbitrary dual node $\tilde{\boldsymbol{n}}_c \in \mathbb{R}^3$ and define $\tilde{\boldsymbol{f}}_e$ as at the end of Section II. The following equality holds:

$$\boldsymbol{u} = \frac{1}{|c|} \sum_{e \in \partial c} (\boldsymbol{u} \cdot \boldsymbol{e}) \, \tilde{\boldsymbol{f}}_e. \tag{10}$$

Proof: Let $\boldsymbol{w} \in \mathbb{R}^3$. Thanks to (2), we have

$$\begin{aligned} 2|c| \, \boldsymbol{u} \cdot \boldsymbol{w} &= 2\int_c \boldsymbol{u} \cdot \boldsymbol{w} \, dV \\ &= \int_c \boldsymbol{u} \cdot \nabla\big(\boldsymbol{w} \times (\boldsymbol{x} - \tilde{\boldsymbol{n}}_c)\big) \, dV \\ &= \int_{\partial c} (\boldsymbol{u} \times \boldsymbol{n}) \cdot \big(\boldsymbol{w} \times (\boldsymbol{x} - \tilde{\boldsymbol{n}}_c)\big) \, dS \\ &= \sum_{f \in \partial c} \int_f (\boldsymbol{u} \times \boldsymbol{n}_f) \cdot \big(\boldsymbol{w} \times (\boldsymbol{x} - \tilde{\boldsymbol{n}}_c)\big) \, dS \\ &= \sum_{f \in \partial c} |f| \, (\boldsymbol{u} \times \boldsymbol{n}_f) \cdot (\boldsymbol{w} \times \tilde{\boldsymbol{e}}_f). \end{aligned} \tag{11}$$

Apply Lemma 1 to every face f in the last term of the above expression, choosing the same node $\tilde{\boldsymbol{n}}_c$ as the arbitrary point involved in the formula. We obtain

$$\begin{aligned}2|c|\, \boldsymbol{u}\cdot\boldsymbol{w} &= \sum_{f\in\partial c}\Big(\sum_{e\in\partial f}(\boldsymbol{u}\cdot\boldsymbol{e})\,(\boldsymbol{b}_e-\tilde{\boldsymbol{n}}_c)\Big)\cdot(\boldsymbol{w}\times\tilde{\boldsymbol{e}}_f)\\ &= \sum_{f\in\partial c}\Big(\tilde{\boldsymbol{e}}_f\times\Big(\sum_{e\in\partial f}(\boldsymbol{u}\cdot\boldsymbol{e})\,(\boldsymbol{b}_e-\tilde{\boldsymbol{n}}_c)\Big)\Big)\cdot\boldsymbol{w}\\ &= \sum_{e\in\partial c}(\boldsymbol{u}\cdot\boldsymbol{e})((\tilde{\boldsymbol{e}}_{f_i}\times(\boldsymbol{b}_e-\tilde{\boldsymbol{n}}_c)-\tilde{\boldsymbol{e}}_{f_j}\times(\boldsymbol{b}_e-\tilde{\boldsymbol{n}}_c))\cdot\boldsymbol{w})\end{aligned} \tag{12}$$

where f_i, f_j are the unique faces of c such that $e = f_i \cap f_j$, for suitable indices $i = i(e)$ and $j = j(e)$, and oriented so that they induce opposite orientations on edge e. Now, dividing by two both members of the last term in (12) and using the definition of $\tilde{\boldsymbol{f}}_e$, it follows that

$$|c|\, \boldsymbol{u}\cdot\boldsymbol{w} = \sum_{e\in\partial c}(\boldsymbol{u}\cdot\boldsymbol{e})\,(\tilde{\boldsymbol{f}}_e\cdot\boldsymbol{w}). \tag{13}$$

Since $\boldsymbol{w}$ is arbitrary, we obtain the claimed equality. □

Theorem 3 (Magic Formulas): Let c be a polyhedral cell. The following tensor identities hold:

$$\sum_{e\in\partial c}\tilde{\boldsymbol{f}}_e\otimes\boldsymbol{e} = |c|\,\mathbb{I}_3 \tag{14}$$

$$\sum_{f\in\partial c}\tilde{\boldsymbol{e}}_f\otimes\boldsymbol{f} = |c|\,\mathbb{I}_3 \tag{15}$$

where $\mathbb{I}_3$ denotes the identity matrix of order 3.

Proof: It is a direct consequence of Theorems 1 and 2. □

IV. Construction of a Consistent Mass Matrix

In this section, we show how the formulas (14) and (15) can be used to construct positive-definite mass matrices $\mathbb{M}^{\mathcal{E}}$ and $\mathbb{M}^{\mathcal{F}}$ for edge and face DoFs, respectively.

Without loss of generality, we assume that the mesh is composed of a single cell c, see Fig. 1. In the general case of a mesh made of more than one cell, the corresponding global mass matrices are obtained by assembling, cell by cell, the contributions from the local matrices $\mathbb{M}_c^{\mathcal{E}}$ and $\mathbb{M}_c^{\mathcal{F}}$ computed for every cell c.

Let us consider a pair of element-wise constant vector fields $\boldsymbol{E}$ and $\boldsymbol{D}$ in a cell c, related by a constitutive relation

$$\boldsymbol{D} = \boldsymbol{\epsilon}\boldsymbol{E} \tag{16}$$

where $\boldsymbol{\epsilon}$ is a reluctivity matrix of order 3 that it is assumed to be symmetric and positive-definite. Then, for the electric voltage along edge e, we write

$$U_e = \boldsymbol{e}\cdot\boldsymbol{E} \tag{17}$$

while the electric flux on $\tilde{f}_e$ is

$$\psi_{\tilde{f}_e} = \tilde{\boldsymbol{f}}_e\cdot\boldsymbol{D}. \tag{18}$$

We say that $\mathbb{M}_c^{\mathcal{E}}$ is a *consistent mass matrix* if

$$\psi_{\tilde{f}_e} = \mathbb{M}_c^{\mathcal{E}}U_e \tag{19}$$

holds exactly for any pair of constant vector fields $\boldsymbol{E}$, $\boldsymbol{D}$ satisfying (16).

Similarly, for magnetic phenomena, we consider a pair of element-wise constant vector fields $\boldsymbol{B}$ and $\boldsymbol{H}$ in a cell c, related by a constitutive relation

$$\boldsymbol{H} = \boldsymbol{\nu}\boldsymbol{B} \tag{20}$$

where $\boldsymbol{\nu}$ is a permittivity matrix of order 3 that it is assumed to be symmetric and positive-definite. Then, for the induction flux on f, we write

$$\phi_f = \boldsymbol{f}\cdot\boldsymbol{B} \tag{21}$$

while the magnetic voltage along $\tilde{e}_f$ is

$$F_{\tilde{e}_f} = \tilde{\boldsymbol{e}}_f\cdot\boldsymbol{H}. \tag{22}$$

We say that $\mathbb{M}_c^{\mathcal{F}}$ is a *consistent mass matrix* if

$$\psi_{\tilde{e}_f} = \mathbb{M}_c^{\mathcal{F}}\phi_f \tag{23}$$

holds exactly for any pair of constant vector fields $\boldsymbol{B}$, $\boldsymbol{H}$ satisfying (20).

An efficient recipe to construct consistent and symmetric mass matrices $\mathbb{M}_c^{\mathcal{E}}, \mathbb{M}_c^{\mathcal{F}}$ combines the geometric identities (14) and (15) with the uniformity of the vector fields in c.

We right multiply (14) by $\boldsymbol{E}$ obtaining

$$\boldsymbol{E} = \frac{1}{|c|}\sum_{e\in\partial c}\tilde{\boldsymbol{f}}_e\,U_e \tag{24}$$

where we have used (17) for U_e; it allows to reconstruct exactly a constant vector field in c, starting from DoFs attached to edges of c. Next, we left multiply (24) by $\boldsymbol{\epsilon}$ and from (16) we write

$$\boldsymbol{D} = \frac{1}{|c|}\sum_{e\in\partial c}\boldsymbol{\epsilon}\tilde{\boldsymbol{f}}_e\,U_e. \tag{25}$$

Finally, using (18), the electric flux becomes

$$\psi_{\tilde{f}_{e'}} = \frac{1}{|c|}\sum_{e\in\partial c}\tilde{\boldsymbol{f}}_{e'}\cdot\boldsymbol{\epsilon}\tilde{\boldsymbol{f}}_e\,U_e \tag{26}$$

and the (e', e) entry of a consistent mass matrix $\mathbb{M}_c^{\mathcal{E}}$ is given by

$$\frac{1}{|c|}\tilde{\boldsymbol{f}}_{e'}\cdot\boldsymbol{\epsilon}\tilde{\boldsymbol{f}}_e \tag{27}$$

with $e, e' \in \partial c$.

Similarly, for magnetic phenomena, we right multiply (15) by $\boldsymbol{B}$ obtaining

$$\boldsymbol{B} = \frac{1}{|c|}\sum_{f\in\partial c}\tilde{\boldsymbol{e}}_f\,\phi_f \tag{28}$$

where we have used (21) for ϕ_f; it allows to reconstruct exactly a constant vector field in c, starting from DoFs attached to faces of c. Next, we left multiply (28) by $\boldsymbol{\nu}$ and from (20) we write

$$\boldsymbol{H} = \frac{1}{|c|}\sum_{f\in\partial c}\boldsymbol{\nu}\tilde{\boldsymbol{e}}_f\,\phi_f. \tag{29}$$

Finally, using (22), the magnetic voltage becomes

$$F_{\tilde{e}_{f'}} = \frac{1}{|c|}\sum_{f\in\partial c}\tilde{\boldsymbol{e}}_{f'}\cdot\boldsymbol{\nu}\tilde{\boldsymbol{e}}_f\phi_f \tag{30}$$

and the (f', f) entry of consistent mass matrix $\mathbb{M}_c^{\mathcal{F}}$ is given by

$$\frac{1}{|c|}\tilde{\boldsymbol{e}}_{f'} \cdot \boldsymbol{v}\tilde{\boldsymbol{e}}_f \tag{31}$$

with $f, f' \in \partial c$.

The matrices $\mathbb{M}_c^{\mathcal{E}}$ and $\mathbb{M}_c^{\mathcal{F}}$ constructed in this way are symmetric, consistent, and positive-semidefinite. To construct positive-definite mass matrices, a possible solution, developed in Theorem 4, is to add to the matrices $\mathbb{M}_c^{\mathcal{E}}$ and $\mathbb{M}_c^{\mathcal{F}}$ a *stabilization matrix*, which is symmetric and positive-semidefinite. The stabilization matrix coincides with the one proposed in the mimetic literature [7].

Theorem 4 (Positive-Definite Local Mass Matrices): Let m be the number of either faces or edges of c. Let $\alpha = (\alpha_1, \ldots, \alpha_{m-3}) \in (\mathbb{R}^+)^{m-3}$ be any $(m-3)$-upla of positive real numbers and let $\mathbb{D}_\alpha$ be the diagonal matrix whose diagonal entries are $\alpha_1, \ldots, \alpha_{m-3}$. Let $\mathbb{E}_c$ and $\mathbb{F}_c$ be two matrices whose rows collect vectors $\boldsymbol{e}$ and $\boldsymbol{f}$ of edges $e \in \partial c$ and faces $f \in \partial c$, respectively. Let $(\boldsymbol{w}_1^{\mathcal{E}}, \ldots, \boldsymbol{w}_{m-3}^{\mathcal{E}})$ be an orthonormal basis of the orthogonal complement of the image space of $\mathbb{E}_c$. Similarly, let $(\boldsymbol{w}_1^{\mathcal{F}}, \ldots, \boldsymbol{w}_{m-3}^{\mathcal{F}})$ be an orthonormal basis of the orthogonal complement of the image space of $\mathbb{F}_c$.

Then, the following matrices:

$$\mathbb{M}_c^{\mathcal{E}} + \sum_{i=1}^{m-3} \alpha_i \boldsymbol{w}_i^{\mathcal{E}} \left(\boldsymbol{w}_i^{\mathcal{E}}\right)^{\mathrm{T}} \tag{32}$$

$$\mathbb{M}_c^{\mathcal{F}} + \sum_{i=1}^{m-3} \alpha_i \boldsymbol{w}_i^{\mathcal{F}} \left(\boldsymbol{w}_i^{\mathcal{F}}\right)^{\mathrm{T}} \tag{33}$$

are symmetric, consistent, and positive-definite.

Proof: It is sufficient to show that (32) is positive-definite. Let $\boldsymbol{z} \in \mathbb{R}^m$ be such that $\boldsymbol{z}^T \mathbb{M}_c^{\mathcal{E}} \boldsymbol{z} = 0$ and $\sum_{i=1}^{m-3} \alpha_i (\boldsymbol{z}^T \boldsymbol{w}_i^{\mathcal{E}})^2 = 0$. Since each α_i is positive, the latter condition implies that $\boldsymbol{z}$ is in the image space of $\mathbb{E}_c$. As a consequence, $\boldsymbol{z} = \mathbb{E}_c \boldsymbol{y}$ for some $\boldsymbol{y} \in \mathbb{R}^3$. It follows that $\boldsymbol{z}^T \mathbb{M}_c^{\mathcal{E}} \boldsymbol{z} = \boldsymbol{y}^T \mathbb{E}_c^T \mathbb{M}_c^{\mathcal{E}} \mathbb{E}_c \boldsymbol{y} = |c|\, \boldsymbol{y}^T \boldsymbol{y} = 0$, where we have used (14). Thus, $\boldsymbol{z} = \mathbb{E}_c \boldsymbol{y} = \boldsymbol{0}$, as desired. □

V. Consequences of Novel Proofs

A first consequence of the novel proofs of the magic formulas, which has been verified by solving patch test problems (i.e. static electromagnetic problems for which the exact solution is piecewise uniform), is that the mass matrices constructed according to Theorem 4 work for very general polyhedral cells. This is a consequence of Theorem 3, which holds for every polyhedral cell c since it is based on Stokes formulas (1) and (2). As an instance, Fig. 3 provides examples of exotic polyhedral cells: concave, not star-shaped, even non-manifold, and non-simply-connected. This generalizes the results in [1], [2], [4] where it is required that polyhedral cells have to be star-shaped.

Another contribution is that each dual node $\tilde{\boldsymbol{n}}_c$ can be placed arbitrarily, even outside the cell c. This observation extends the standard geometric construction of the barycentric dual grid, where a dual node $\tilde{\boldsymbol{n}}_c$ is assumed to be fixed and equal

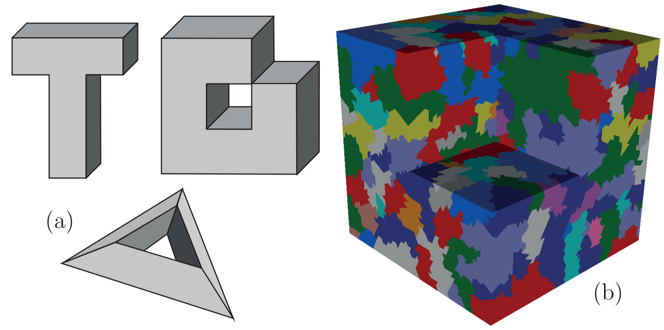

Fig. 3. (a) Examples of concave, non-manifold and non-simply-connected mesh elements. (b) Polyhedral grid obtained with *adaptive coarsening* [9] where exotic elements are constructed by gluing tetrahedra of a background simplicial mesh.

to the barycenter $\boldsymbol{b}_c$ of c. We point out that this does not affect the role of geometric elements of the barycentric dual grid in the expressions of balance laws of physical theories. This is because, although dual edges and dual faces are stretched and deformed by using an arbitrary dual node $\tilde{\boldsymbol{n}}_c$, they still provide a valid dual grid structure.

VI. Conclusion

In the present contribution, novel proofs of the magic formulas are given. These are based on Stokes formulas and show that mass matrices constructed starting from them work for very general polyhedral elements and arbitrarily positioned dual nodes. Future research may investigate how to choose dual nodes in order to optimize mass matrices, as measured by suitable objective functions. In this case, optimal dual nodes may lie outside elements and our contribution shows that these still provide a feasible dual grid structure.

References

[1] L. Codecasa and F. Trevisan, "Constitutive equations for discrete electromagnetic problems over polyhedral grids," *J. Comput. Phys.*, vol. 225, no. 2, pp. 1894–1918, Aug. 2007.
[2] L. Codecasa, R. Specogna, and F. Trevisan, "A new set of basis functions for the discrete geometric approach," *J. Comput. Phys.*, vol. 229, no. 19, pp. 7401–7410, Sep. 2010.
[3] F. Brezzi, K. Lipnikov, and V. Simoncini, "A family of mimetic finite difference methods on polygonal and polyhedral meshes," *Math. Models Methods Appl. Sci.*, vol. 15, no. 10, pp. 1533–1551, Oct. 2005.
[4] J. Bonelle, D. A. Di Pietro, and A. Ern, "Low-order reconstruction operators on polyhedral meshes: Application to compatible discrete operato schemes," *Comput. Aided Geometric Des.*, vols. 35–36, pp. 27–41, May 2015.
[5] T. Tarhasaari, L. Kettunen, and A. Bossavit, "Some realizations of a discrete hodge operator: A reinterpretation of finite element techniques [for EM field analysis]," *IEEE Trans. Magn.*, vol. 35, no. 3, pp. 1494–1497, May 1999.
[6] A. Bossavit, *Computational Electromagnetism: Variational Formulations, Complementarity, Edge Elements*. London, U.K.: Academic, 1998.
[7] K. Lipnikov, G. Manzini, and M. Shashkov, "Mimetic finite difference method," *J. Comput. Phys.*, vol. 257, pp. 1163–1227, Jan. 2014.
[8] E. Tonti, *The Mathematical Structure of Classical and Relativistic Physics: A General Classification Diagram*. New York, NY, USA: Springer, 2013.
[9] D. A. Di Pietro and R. Specogna, "An a posteriori-driven adaptive mixed high-order method with application to electrostatics," *J. Comput. Phys.*, vol. 326, pp. 35–55, Dec. 2016.